

ADVANCED CHARACTERIZATION METHODS FOR TRISO FUELS

A. K. Kercher, J. D. Hunn, J. R. Price, G. E. Jellison, F. C. Montgomery, R. N. Morris,
J. M. Giaquinto, D. L. Denton
Oak Ridge National Laboratory, Oak Ridge, TN, USA

Abstract

Ongoing research at Oak Ridge National Laboratory focuses on updating fuel characterization methods to support fuel development efforts, qualify TRISO fuels for irradiation testing at the Idaho National Laboratory Advanced Test Reactor (INL-ATR), and to establish a new standard for particle fuel characterization in the US. Computer automated microscopy and analysis have allowed particle size, particle shape, and layer thicknesses to be easily and accurately measured for large samples sizes. Preferred orientation in the pyrocarbon layers is being rigorously measured by sophisticated ellipsometry methods. Density column procedures have been refined based on a physical understanding of the underlying mechanisms. Modern microwave digestion methods are being applied to supplement traditional Leach-Burn-Leach measurements.

Introduction

Ongoing research at Oak Ridge National Laboratory focuses on producing candidate TRISO particle fuels for testing at the Idaho National Laboratory Advanced Test Reactor (INL-ATR). Extensive characterization of kernels, TRISO-coated particles, and compacts is required before insertion of the candidate fuels into the test reactor. Approximately sixty separate qualification tests are required to qualify the kernels, coated particles, and compacts of each candidate TRISO fuel.

The fuel characterization effort focuses on updating fuel characterization methods to properly qualify TRISO fuels for AGR testing and to establish a new standard for particle fuel characterization in the US. Using historical characterization programs and techniques as a starting point, every aspect of TRISO fuel characterization has been revisited. A few of these characterization methods will be discussed herein: optical microscopy, anisotropy measurements, density column, and impurity leaching.

Computer automated optical microscopy

Optical microscopy is used for characterizing and qualifying kernel size, kernel shape, layer thicknesses, coated particle size, and coated particle shape. Shadow images are used to obtain the overall size and shape of kernels or coated particles. Shadow images are formed by backlighting a layer of particles on a microscope stage to create shadow outlines of kernels or coated particles for micrographs. Cross-sectional images are used to obtain layer thicknesses in coated particles.

The conventional microscopy technique has shadow images or cross-sections imaged individually and measured by hand or measured “manually” with a computer. Manual microscopy is time-consuming and tedious. The number of measurements per item (kernel or coated particle) must be minimized in order to allow for analysis of moderately large samples in a reasonable amount of time. Practical sample sizes are generally 50-100 particles. For shadow images, each particle in the sample has “diameter” measurements performed to determine mean particle diameter and/or diameter aspect ratio (D_{\max}/D_{\min}). For cross-sections, mean thickness for each layer is often determined from a few layer thickness measurements for each particle.

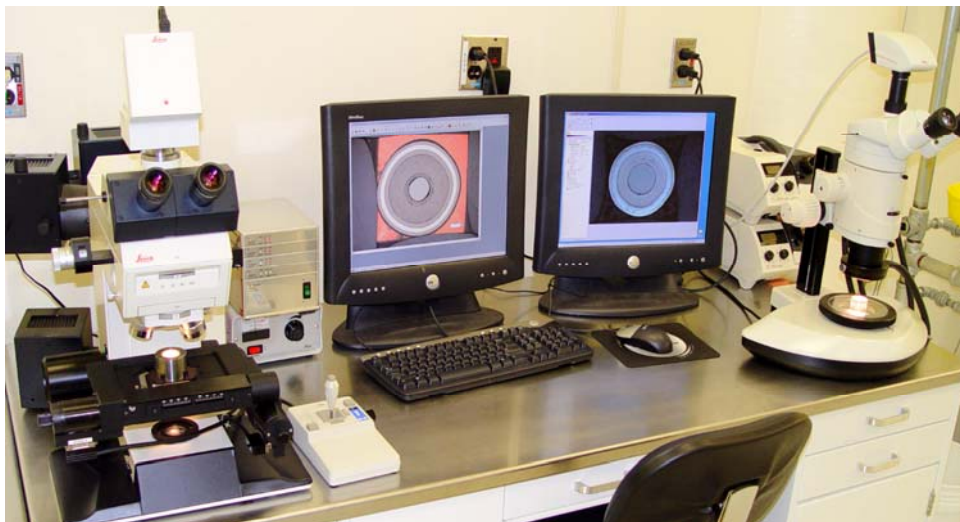


Figure 1: Computer automated optical microscopy system.

At ORNL, computer automated optical microscopy is used to analyze large samples quickly and easily (Figure 1). A Leica DMRX optical microscope is equipped with a computer-driven stage and a digital image acquisition system. For shadow images, the stage automatically moves to allow for a tiled array of pictures to be generated over a large area of kernels/particles. Sample sizes of 2000-5000 particles are routinely examined as shadow images on this microscopy system. For cross-sections, particles are placed in a mesh, mounted, and polished using standard metallographic techniques. Having particles mounted in a mesh allows for automated picture acquisition using a computer-driven stage which automatically moves to each grid position and acquires an image. Polished mounts with 99 particles each are common for cross-sections; practical sample sizes are ~100-300 particles. Digital micrographs are analyzed by image analysis (IA) software that was written in-house [1]. For shadow images, IA software can identify individual particles, locate particle centers, measure the radial distances to the particle edge at 1° intervals, and determine an analytical fit for the shape of the particle's shadow based on Fourier transforms (Figure 2). This detailed data set *for each particle* can be used to generate a wide variety of descriptive statistics (e.g., mean radius, mean diameter, radius standard deviation, radius aspect ratio, diameter aspect ratio, curvature). For cross-sections, IA software can identify kernels, locate kernel centers, radially unfold the image, measure the radial distances to all layers at 1° intervals, and perform an "off-midplane" correction (Figure 3). The large number of position measurements for each layer allows for accurate determination of mean layer thicknesses for each particle.

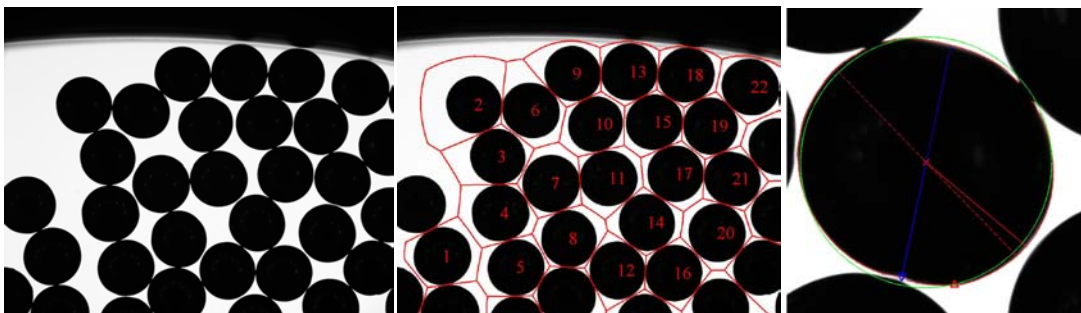


Figure 2: Image analysis software identifies individual particles from digital images, locates the particle centers, measures radial distances to the particle edge, and reports key parameters.

Computer automated microscopy is more reproducible and is generally more accurate than manual microscopy methods. For each particle, mean radius and/or mean layer thickness can be calculated based upon hundreds of automated measurements instead of a handful of manual measurements. The diameter aspect ratio depends upon accurately identifying and measuring the minimum and maximum diameter of a particle's shadow image. Manual identification of minimum and maximum diameters is inconsistent and often, for convenience sake, minimum and maximum diameters are estimated to be perpendicular to each other. Automated measurement of diameters at 1° intervals allows for unbiased identification of minimum and maximum diameters. The definition of a boundary (particle edge or layer boundary) can be strictly defined using computer automated microscopy to provide consistent results. Manual microscopy is prone to operator biases when identifying boundaries.

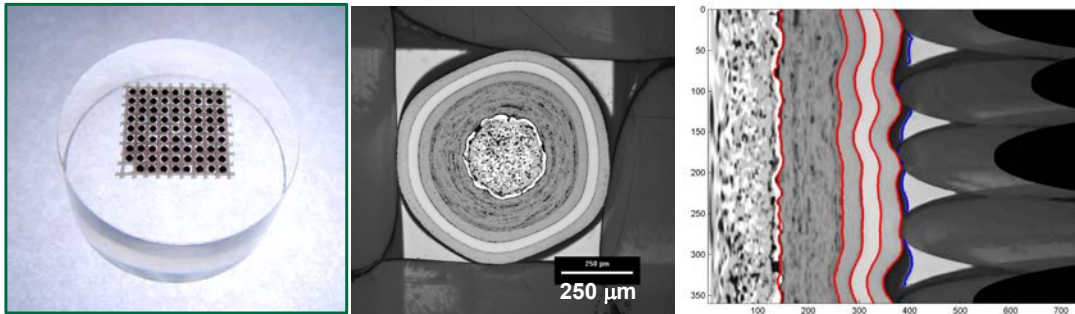


Figure 3: For cross-sectional images, particles are mounted inside a mesh. This organized array of particles allows for computer automated image acquisition and analysis. The radially unwrapped image shown at far right illustrates how coating thickness varies around the particle.

Computer automated microscopy allows for a larger sample size, which greatly benefits qualification and statistical description of kernels and fuel. For shadow images, computer automated microscopy allows for a sample size that is approximately 100 times larger than feasible by manual measurement. The standard deviation of a mean is inversely proportional to the square root of the sample size. Thus, the standard deviation of the mean is 10 times smaller for computer automated microscopy than for manual microscopy. Sample size is particularly important for fuel qualification based on attribute testing, such as the specification for diameter aspect ratio.

Table 1: A hypothetical specification for the diameter aspect ratio of kernels.

Property	Control Limit	Tolerance Limit (L_T)	Confidence Level
Diameter Aspect Ratio (kernels)	≤ 1.05	0.1	0.95

Consider the hypothetical specification for the diameter aspect ratio of kernels shown in Table 1. A sample size of 50 could be used to test whether a sample passes the specification, but the defect fraction of the lot (fraction of material in the lot that is outside the control limit) would have to be 0.0072 or less to have a 95% chance of passing the specification with a sample size of 50. If a sample size of 5000 was used, then the defect fraction of the lot would have to be 0.086 or less to have a 95% chance of passing the specification with a sample size of 5000. In order to have a significant probability of passing a specification, a small sample size requires a higher quality material than a large sample size.

Collection of data at 1° intervals allows for detailed description of individual particles. For example, in addition to the average thickness of a particle's layer, the standard deviation in a particle's layer thickness can be readily determined. Because of the data collection method, computer automated microscopy can provide radius aspect ratios and other alternate measures of shape. Diameter aspect ratio is excellent for describing the shape of ellipses, but it does a poor job of describing asymmetric shapes because the "nondefective" end of a diameter affects the reported aspect ratio. Radius aspect ratio is equally descriptive of symmetric and asymmetric shapes. Radius aspect ratios tend to be significantly higher than diameter aspect ratios for non-spherical faceted particles.

The large amount of data collected by automated methods around each boundary allows for Fourier analysis techniques to be used to generate a function describing the boundary shape. An

equation for the boundary allows additional parameters, such as the curvature, to be calculated for the points around the boundary. Having an equation for the boundary allows local features to be identified.

Diameter aspect ratio is the established metric to describe shape for kernels and coated particles. Computational methods have shown that local deviations from a spherical shape can result in stress risers that can increase the fuel failure rate during irradiation. To date, a diameter aspect ratio metric has not been shown to strongly correlate with particle fuel failure. Historically, diameter aspect ratio has been used only because it could be readily measured; better metrics are desired.

A new metric for particle shape has been developed at ORNL: the product of the radius and curvature at the point of maximum curvature ($r\kappa_{\max}$). This metric is unitless and, in a membrane theory approximation, can be related to layer stresses. The sharpness of corners on a fuel particle can be correlated to layer stress increases and possible out-of-shell loading (“bending forces”) possibly leading to failure in a TRISO layer. The maximum radius-curvature product of a particle relates to the sharpest feature (corners). Note that an aspect ratio and $r\kappa_{\max}$ are fundamentally different measures of shape (Figure 4). The aspect ratio is a global approximation of ellipticity. The $r\kappa_{\max}$ metric is related to localized stresses. Computer automated microscopy allows calculation of several different measures of shape, but the key is to choose a simple metric that can be related to a probable failure mechanism.

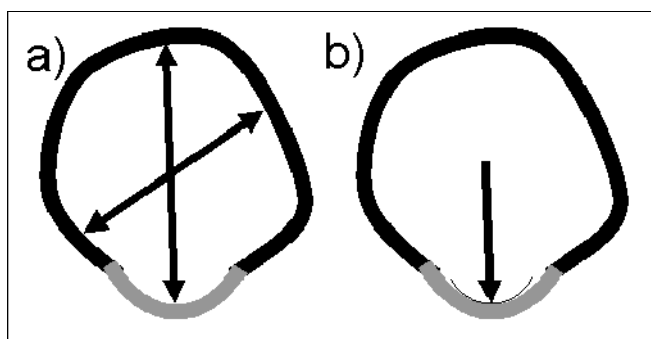


Figure 4: Diameter aspect ratio (a) provides a measure of general shape. The new metric, $r\kappa_{\max}$, (b) provides a measure of the sharpest feature that the particle exhibits.

Anisotropy of pyrocarbons

Designing pyrocarbons for TRISO fuels generally involves a trade-off. A pyrocarbon with a high density often has low porosity and an anisotropic microstructure. A pyrocarbon with a low density often has high porosity and a relatively disordered carbon structure. Porosity that extends through a pyrocarbon layer results in a highly permeable pyrocarbon layer. An anisotropic carbon layer exhibits significant dimensional change during irradiation, which can lead to coating failure. Thus, the goal is to produce a pyrocarbon with a sufficiently high density to have low permeability and a sufficiently isotropic microstructure to avoid excessive dimensional change during irradiation.

Conventionally, an optical polarimeter or microellipsometer has been used to evaluate the anisotropy of pyrocarbon layers. Neither technique can probe all of the possible optical interactions that pyrocarbon can have with incident polarized light (as described by a Mueller matrix). As a result, neither conventional technique can provide sufficient data to fully probe the anisotropy of pyrocarbon material. Current research at ORNL uses a two-modulator generalized ellipsometry microscope (2-MGEM) (Figure 5). The 2-MGEM can capture all eight Mueller matrix parameters pertinent to

pyrocarbons [2]. Therefore, the 2-MGEM can fully probe the optical anisotropy of pyrocarbon material. Important data outputted from the 2-MGEM are diattenuation (N), retardation (δ), fast axis angle, and circular diattenuation. The maximum optical resolution of the 2-MGEM is $\sim 4 \mu\text{m}$ with a time per measurement point of 0.2-0.5 seconds.

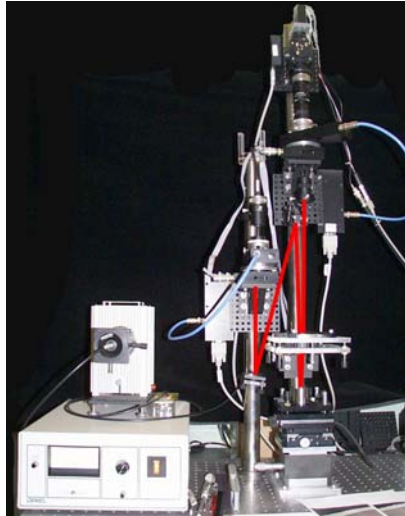


Figure 5: A picture of the two-modulator generalized ellipsometry microscope (2-MGEM).

The 2-MGEM system has several advantages over conventional techniques. All pertinent Mueller matrix parameters can be measured. Nonspecular reflections and any other light not transmitted to the detector do not affect the accuracy of the measurement. The instrument resolution allows for identification of any localized anisotropy features through the thickness of pyrocarbon layers (Figure 6). Because of measurement accuracy and elimination of conventional sources of measurement error, the 2-MGEM can measure anisotropies that are 10 times smaller than conventional techniques.

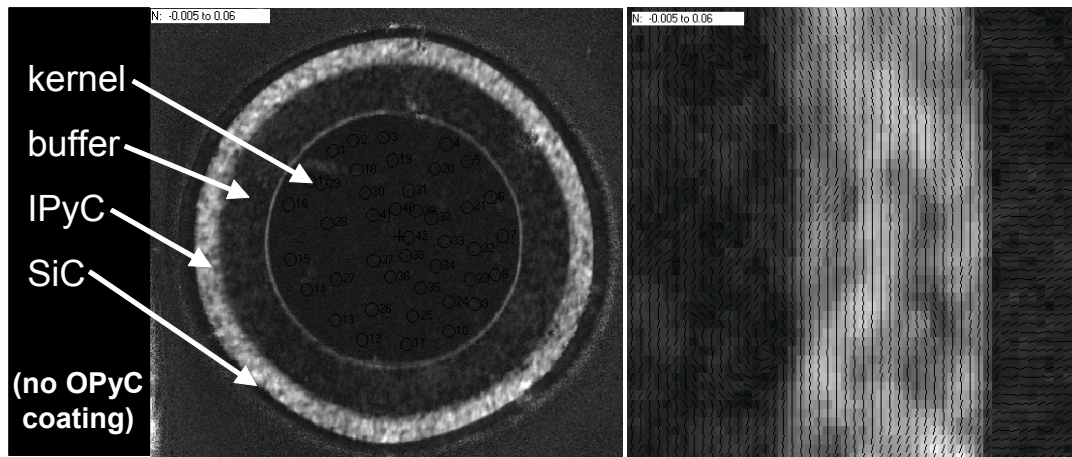


Figure 6: High resolution images from the 2-MGEM system ($2\mu\text{m}$ spatial resolution). Diattenuation grayscale goes from -0.005 to 0.06. Significant diattenuation in the IPyC layer makes it appear as a bright ring in the image. The lines in the rightmost picture indicate the fast axis orientation.

Density column

In AGR fuel characterization and qualification, a density column is used to characterize the density of IPyC, SiC, and OPyC layer fragments. Variability in layer density may exist from particle to particle of the same batch, so the mean density and dispersion are specified in AGR fuel specifications. A density column is constructed to have a nearly linear density gradient. Material of unknown density is dropped in the column and compared to the float position of known standards [3].

Figure 7 shows a schematic illustration of how a density column is constructed. Initially, two fluids with densities that span the desired measurement range are poured into the two beakers. Fluid from beaker 1 is transferred into beaker 2 at a constant rate (r_1). Fluid from beaker 2 is transferred into the column at a constant rate (r). Flow rate into the column is controlled by a peristaltic pump. Flow rate between beakers is controlled by another peristaltic pump or by gravity feed. Starting from equilibrium, gravity feed rate is roughly half the flow rate into the column, but can be significantly affected by the fluid viscosity, beaker fluid heights, the current fluid density in beaker 2, and other practical set-up issues.

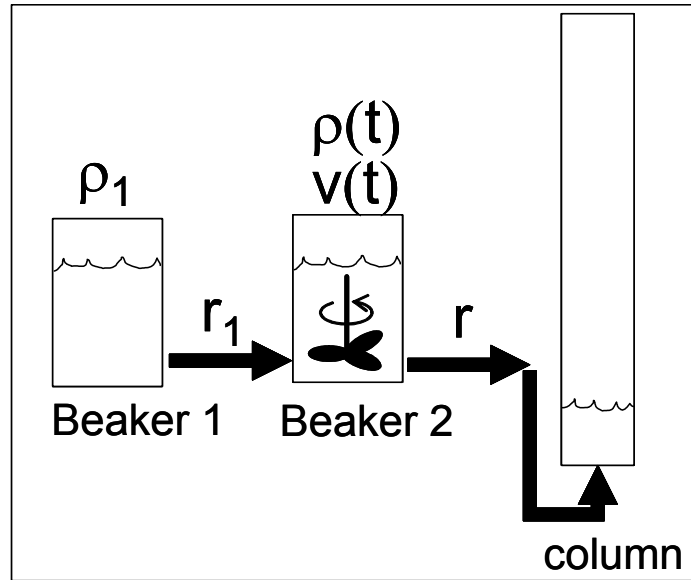


Figure 7: Schematic illustration of how a density column is filled.

The key to quality density column measurements is producing a sufficiently linear column over the desired density range. It is important to maintain constant flow rates at the proper ratio. The mathematical derivation, shown below, indicates the relative flow rates necessary to obtain a linear column and can calculate the resultant density profile.

$$\frac{d\rho}{dt} = \frac{d}{dt} \left(\frac{w}{v} \right) = \frac{1}{v} \frac{dw}{dt} - \frac{w}{v^2} \frac{dv}{dt} = \frac{1}{v} \frac{dw}{dt} - \frac{\rho}{v} \frac{dv}{dt} \quad \text{Eq. 1}$$

where $\rho(t)$ is the fluid density in beaker 2, ρ_1 is the fluid density in beaker 1, $v(t)$ is the volume of fluid in beaker 2, $w(t)$ is the fluid weight in beaker 2, and t is time. The following equations can be derived from mass balance considerations and an assumption of zero volume change due to mixing.

$$v(t) = v(0) + (r_1 - r)t \quad \text{Eq. 2}$$

$$\frac{dv}{dt} = r_1 - r \quad \text{Eq. 3}$$

$$\frac{dw}{dt} = r_1 \rho_1 - r \rho \quad \text{Eq. 4}$$

where $v(0)$ is the initial volume in beaker 2. Combining Eq. 1, 3, & 4 and rearranging terms obtains the following differential equation.

$$\frac{d\rho}{dt} + \frac{r_1}{v} \rho = \frac{r_1}{v} \rho_1 \quad \text{Eq. 5}$$

This first-order differential equation can be solved by the method of integrating factors to obtain the solution:

$$\rho = \rho_1 + C_1 v^{r_1/r-r_1} \quad \text{Eq. 6}$$

where C_1 is a constant of integration. To get a linear density column, $d\rho/dt$ must be constant.

$$\frac{d\rho}{dt} = C_1 \left(\frac{r_1}{r-r_1} \right) v^{2r_1-r/r-r_1} \frac{dv}{dt} = C_1 \left(\frac{r_1}{r-r_1} \right) (r_1-r) v^{2r_1-r/r-r_1} = -C_1 r_1 v^{2r_1-r/r-r_1} \quad \text{Eq. 7}$$

Notice that, for the derivative to be constant (Eq. 7), the flow rate between beakers must be half of the flow rate into the column ($r = 2r_1$). Using the initial conditions (at $t = 0$, $\rho = \rho(0)$ and $v = v(0)$), the final equation for the density column can be derived to be:

$$\rho = \rho(0) + \frac{\rho_1 - \rho(0)}{v(0)} r_1 t \quad \text{Eq. 8}$$

where $r_1 t$ is a function of the vertical position in the column assuming the column has a uniform cross-section. Using Eq. 8, linear density columns can be constructed with the desired density range occurring over the measurable position range.

The methods of transferring fluid should be chosen to have constant flow rates in the proper ratio. A flow controller (e.g., peristaltic pump) is recommended to control the flow rate into the column. Gravity feed can be adequate for controlling the flow rate between beakers when the starting fluids have similar densities (i.e., narrow density range in final column). A flow controller should be used for controlling the flow rate between beakers when constructing a column with a relatively wide density range. By considering the practical implications of Equations 7 and 8, density columns have become more predictable, more linear, and consequently more accurate.

Impurity leaching

Impurity analysis of compacts generally involves the dissolution of compact impurities in a harsh acidic solution (such as a refluxing acid bath) over a period of several hours and the impurity analysis of the leachate by a technique such as atomic emission spectroscopy. Impurities of particular interest in compacts of TRISO particles include aluminum, calcium, chromium, cobalt, manganese, nickel, titanium, and vanadium. Typical specifications range from about 25 μg to 500 μg of a certain impurity per compact.

Research at ORNL has begun to evaluate using microwave digestion for dissolution of compact impurities. The microwave digestion system at ORNL uses fluoropolymer-lined pressure vessels and microwave heating to dissolve impurities at elevated temperature and pressure. Relatively small quantities of acid are required to dissolve impurities in a compact. For a ~ 12.34 mm diameter compact that is ~ 25.4 mm long, approximately 10 mL of acid is required per sample. A refluxing acid bath is

limited by the boiling point of the acid, but the microwave digestion system is only limited by the pressure vessel liner. Common temperatures for the microwave digestion system are 170-210°C. The high temperature results in dissolution times of approximately 10 minutes. The microwave digestion system has a carousel that allows up to 10 pressure vessels to be run simultaneously (Figure 8).



Figure 8 The microwave digestion system can simultaneously heat a carousel of ten fluoropolymer-lined pressure vessels. A disassembled pressure vessel is shown.

Preliminary tests have been conducted. Compacts of matrix were doped with iron, manganese, nickel, chromium, and cobalt. Using microwave digestion in nitric acid at 170°C for 10 minutes, a high percentage (~70-100%) of the added Fe, Mn, Ni, and Co were found in the leachate (using inductively coupled plasma atomic emission spectroscopy (ICP-AES)). Dissolution of chromium was low using only nitric acid (less than 20%). The acid and temperature are currently being modified to improve the dissolution of the impurities, but these preliminary tests provided promising results.

Summary

New and modified characterization techniques for kernels, TRISO particles, and compacts are being developed at ORNL. Computer automated optical microscopy is being used to analyze large samples quickly and easily. Image analysis software written at ORNL can provide hundreds of radius or layer thickness measurements per particle, which more thoroughly characterizes each particle and has enabled the development of new metrics to describe key particle characteristics. A two-modulator generalized ellipsometry microscope is being used to accurately measure the optical anisotropy of pyrocarbon coatings with a sensitivity and resolution that exceeds commonly used optical polarimeters or microellipsometers. A straightforward mathematical analysis has provided insights into how to construct density columns that are more predictable, more linear, and more accurate. Research has recently begun to evaluate microwave digestion for dissolution of compact impurities. Microwave digestion offers the potential to rapidly dissolve impurities from compacts using small quantities of acid. Preliminary results on microwave digestion of doped compacts have been promising.

References

- [1] Price J, Hunn J. Optical inspection of coated particle nuclear fuel. in Proceedings of Machine Vision Applications in Industrial Inspection XII, SPIE 2004, vol. 5303: 137-149.
- [2] Jellison GE. Generalized ellipsometry for materials characterization. Thin Solid Films 2004; 450(1):42-50.
- [3] American Society for Testing and Materials. 2004 Annual Book of ASTM Standards, D1505-03.